Available online at www.sciencedirect.com
SCIENCE DIRECT®
Journal of Molecular Catalysis A: Chemical 216 (2004) 223–231
JOURNAL OF MOLECULAR CATALYSIS A: CHEMICAL
www.elsevier.com/locate/molcata

An investigation of the adsorption of (*R*,*R*)-tartaric acid on oxidised Ni{1 1 1} surfaces

T.E. Jones, C.J. Baddeley*

School of Chemistry, University of St. Andrews, St. Andrews, Fife KY16 9ST, UK

Available online 24 April 2004

Abstract

Despite extensive research into the heterogeneously catalysed enantioselective hydrogenation of β-ketoesters over chirally modified Ni-based catalysts, the surface chemistry underlying enantioselective promotion is still poorly understood and hotly debated. In recent years, surface scientists have made considerable strides in understanding how chiral modifiers such as (*R*,*R*)-tartaric acid interact with metal surfaces. However, all of the research to date has concentrated on clean metal surfaces. Since modification of Ni nanoparticles occurs from aqueous solution and since the metallic nanoparticles are normally exposed to air prior to modification, it is likely that the adsorption of chiral modifiers occurs on Ni surfaces covered by a passivating oxide/hydroxide film. In this paper we investigate, with RAIRS and TPD, the adsorption of (*R*,*R*)-tartaric acid on Ni{1 1 1}; Ni{1 1 1}–p(2 × 2)O and Ni{1 1 1}–NiO{1 1 1} surfaces. We show that the thermal stability of the adsorbed tartrate species is strongly enhanced by oxidation of the Ni surface. Indeed, the thermal decomposition of the film is shown to tend towards that expected for nickel(II)tartrate. We investigate the effect of preoxidising and/or thermal processing of the Ni surfaces on the vibrational spectra of the adsorbed chiral modifier. The implications of this work for promoting the understanding of enantioselective heterogeneous catalysis are discussed.

Keywords: (*R*,*R*)-Tartaric acid; Chiral; Catalysis; Surface; Nickel

1. Introduction

One of the biggest challenges facing heterogeneous catalysis in the 21st century is to break into the field of industrial chiral catalysis. The importance of this type of catalysis is perhaps best emphasised by the award of the 2001 Nobel Prize for Chemistry to Knowles, Noyori and Sharpless for their work in homogeneously catalysed enantioselective catalysis [1]. For example, Knowles work at Monsanto led to the first industrial scale asymmetric synthesis—the production of L-DOPA used in the treatment of Parkinson's Disease.

Two heterogeneously catalysed chiral reactions have been the subject of particularly extensive research—the hydrogenation of α-ketoesters over Pt-based catalysts and β-ketoesters over Ni-based systems. These catalytic reactions share many common features and have been the subject of a number of review articles [2–6]. The key step in enabling the catalysts to behave enantioselectively is the adsorption, from solution, of chiral molecules (modifiers) onto the surface of the supported metal nanoparticles. In the Pt case, successful modifiers include the cinchona alkaloids (e.g. cinchonidine). Successful modifiers appear to require two particular characteristics. The first requirement is an aromatic ring system (naphthalene or quinoline) which is thought to anchor the modifier to the Pt surface. Secondly, the functional group attached to the aromatic system needs to contain a nitrogen atom capable of interacting with the β-ketoester reagent, e.g. via a H-bonding interaction. Two types of mechanism have been proposed to explain the surface chemistry underlying the enantioselective behaviour. In the Pt case, a "Template" model was proposed by Wells and co-workers [7] which suggested that the adsorption of chiral modifiers (typically cinchona alkaloids such as cinchonidine) resulted in the formation of ordered overlayers analogous to those produced by the adsorption of naphthalene on Pt{1 1 1} (the alkaloids possess a similar aromatic moiety to naphthalene) [8]. If this was the case, then the chirality of the alkaloid adsorbate was proposed to create chiral "environments" which may favour adsorption

* Corresponding author. Tel.: +44-133-4467236; fax: +44-133-4463808.
E-mail address: cjb14@st-and.ac.uk (C.J. Baddeley).

1381-1169/$ – see front matter © 2004 Elsevier B.V. All rights reserved.
doi:10.1016/j.molcata.2004.03.017

by one face of the prochiral reactant which may account for the enantioselectivity observed in the catalytic reaction. An alternative model was proposed [2,6] whereby a hydrogen bonding interaction between the ketone group of the reagent and the N-atom of the quinuclidine moiety of the alkaloid molecule was considered to be sufficient to cause enantioselectivity. The fact that no evidence has been found for ordered structures on single crystal Pt surfaces following the adsorption of cinchonidine and similar molecules [9,10] has led to the second model being widely accepted in the catalytic community. This is further supported by the observation, with STM, of 1:1 modifier-reactant complexes by Lambert and co-workers [10].

In the Ni catalysed system, the generally accepted model for chiral behaviour was, for many years, considered to be a 1:1 interaction model [2–6] with H-bonding occurring between the adsorbed modifier (typically α-hydroxy acids such as (*R*,*R*)-tartaric acid or α-amino acids such as (*S*)-alanine) and the reagent stabilising a particular reagent configuration on the surface. In the late 1990s, Ortega Lorenzo et al. [11] proposed that a "Template" model may be important in this catalytic system. (*R*,*R*)-tartaric acid was found have an extremely strong tendency to form a range of ordered structures on Cu{1 1 0}. Some of these structures resulted in the whole surface becoming chiral with an extended network of (*R*,*R*)-tartaric acid species (adsorbed as bitartrate). The adsorbate structures produced were exactly mirrored when similar experiments were carried out with (*S*,*S*)-tartaric acid [12]. The behaviour of (*R*,*R*)-tartaric acid on Ni surfaces has also been investigated. Humblot et al. [13] found no evidence for ordered arrangements of (*R*,*R*)-tartaric acid on Ni{1 1 0}. By contrast, Jones and Baddeley [14] discovered two discrete ordered arrangements in the Ni{1 1 1} system with local coverages of 0.20 and 0.18 ML. Attempts to investigate the interaction of methylacetoacetate (MAA) with these ordered structures showed that methylacetoacetate did not stick to the chirally modified surface at 300 K. However, when MAA was dosed onto a low coverage (*R*,*R*)-tartaric acid overlayer (where no short or long range order was observed with STM), a remarkable 2-D co-crystalline structure was observed to form [15]. This adlayer structure appeared to consist of an ordered arrangement of one-to-one complexes of adsorbed tartrate and MAA. Submolecular resolution imaging of this structure showed that each MAA species was adsorbed in an identical environment. Furthermore, hydrogenation of this species would result in the formation of the (*R*)-form of methyl-3-hydroxybutyrate (the product observed in the enantioselective reaction). This led to the proposal of a new model for this catalytic reaction which does not require the presence of pre-adsorbed ordered arrays of modifiers. The geometry of the adsorbed MAA species appears to be stabilised by (i) a direct interaction with a tartrate species and (ii) by being surrounded by an ordered arrangement of 1:1 complexes.

Until now, the UHV-based work investigating the Ni catalysed system has concentrated on the chemisorption of chiral modifiers on metallic surfaces. However, chiral modification occurs from aqueous solution and, in the majority of cases, no attempt is made to exclude air from the catalyst samples prior to modification. It is well known that exposure of Ni surfaces to air results in the formation of passivating oxide layers (e.g. [16]) and similarly exposure to water vapour or aqueous conditions results in the formation of hydroxide terminated surfaces. In this study, we have attempted to model the interaction at the liquid–solid interface by investigating the adsorption of (*R*,*R*)-tartaric acid on two distinct oxidised surfaces—Ni{1 1 1}–p(2 × 2)O and Ni{1 1 1}–NiO{1 1 1}. These data are then compared with those acquired from the Ni{1 1 1}–(*R*,*R*)-tartaric acid system [14].

We report the use of TPD and RAIRS to characterise the adsorption of (*R*,*R*)-tartaric acid on oxidised Ni surfaces as functions of adsorbate coverage and sample temperature. We will compare the behaviour with that observed on Ni{1 1 1} and discuss the relevance of our work to chiral catalysis.

2. Experimental

Two ultrahigh vacuum (UHV) chambers were used in this study. RAIRS experiments were carried out in an Omicron UHV system with a base pressure of 1×10^{-10} mbar which also has facilities for sample cleaning and LEED/AES/STM experiments. A Nicolet FTIR spectrometer fitted with a N_2(l) cooled mercury cadmium telluride (MCT) detector was used to collect RAIRS data. The second UHV system has a base pressure of $\sim 3 \times 10^{-10}$ mbar and has facilities for sample cleaning, a QMS for TPD experiments and a four-grid RFA for LEED/AES experiments. The TPD experiments were carried out using a heating rate of $\sim 3\,\mathrm{K s^{-1}}$.

The Ni{1 1 1} sample was cleaned by cycles of Ar^+ bombardment (1.5 keV) and annealing to 900 K until a sharp (1 × 1) LEED pattern was obtained and no impurities were observed by AES. Two oxidised systems were studied, the first was the Ni{1 1 1}–p(2 × 2)O (0.25 ML) surface created by a 5 L exposure of oxygen at 373 K [17]. The second system involved a much higher oxygen dose (600 L O_2 at 373 K) which gave rise to a LEED pattern characteristic of the Ni{1 1 1}–NiO{1 1 1} surface [18]. The samples were exposed to (*R*,*R*)-tartaric acid via sublimation of the solid acid from a glass tube heated to ∼145 °C as measured by a thermocouple embedded in the solid.

3. Results

3.1. TPD

The primary desorption products observed in TPD experiments occurred at masses 2 (H_2), 18 (H_2O), 28 (CO) and 44 (CO_2). At no stage was molecular (*R*,*R*)-tartaric acid observed to desorb from the surface. For each of the four TPD experiments shown in Fig. 1a–d, a 900 s (*R*,*R*)-tartaric

acid dose was used as this dose was found to result in the formation of a saturated monolayer of adsorbed tartrate in each case.

Fig 1a shows the desorption products following a 900 s (*R*,*R*)-tartaric acid dose onto clean Ni{1 1 1} at 300 K. Desorption of mass 2 (H_2) is observed in two peaks with T_{max} values of ~375 and 420 K. The desorption of H_2O occurs in one, asymmetric, peak with a T_{max} of ~420 K and a prominent tail at higher temperatures. Similarly CO desorption occurs primarily in a peak at 420 K with a low temperature shoulder and an additional, smaller, peak at higher temperature. Finally, CO_2 desorption occurs in two

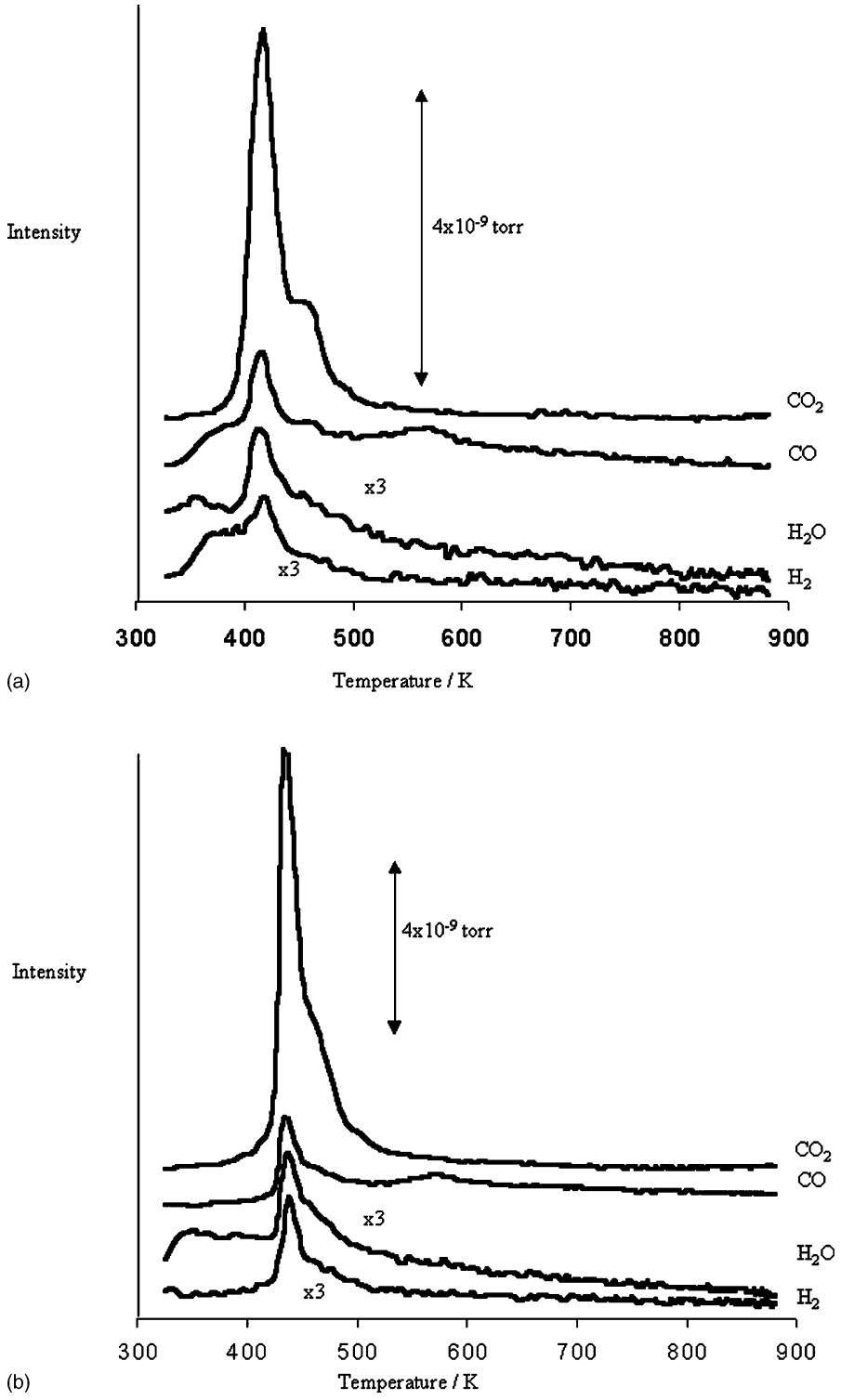

Fig. 1. TPD of a 900 s (*R*,*R*)-tartaric acid dose on (a) Ni{1 1 1} at 300 K; (b) Ni{1 1 1} at 350 K; (c) Ni{1 1 1}–p(2 × 2)O at 300 K and (d) NiO–Ni{1 1 1} at 300 K.

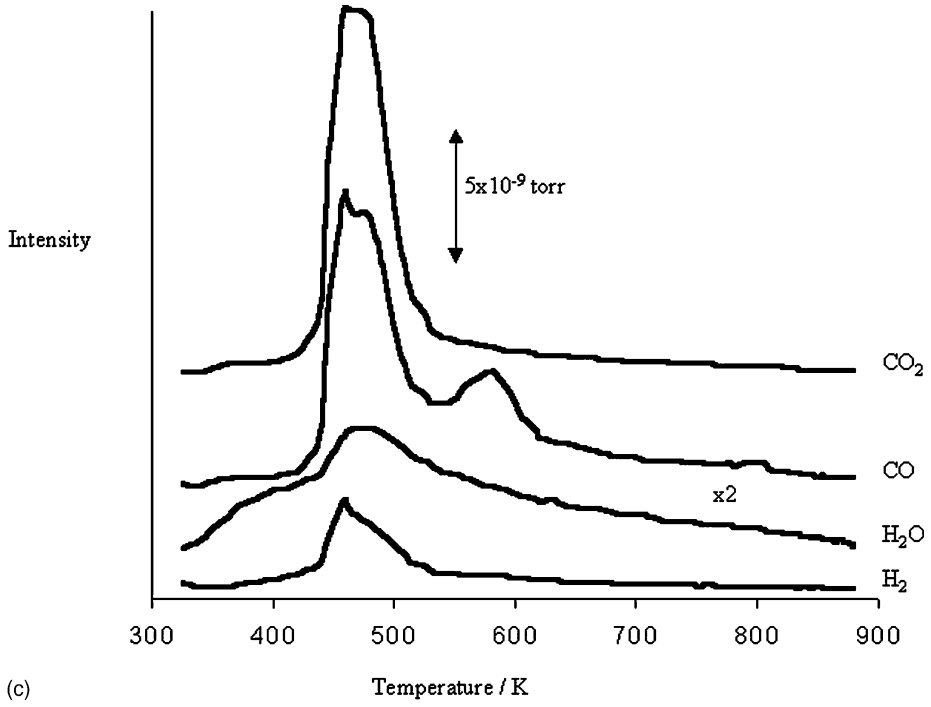

(c)

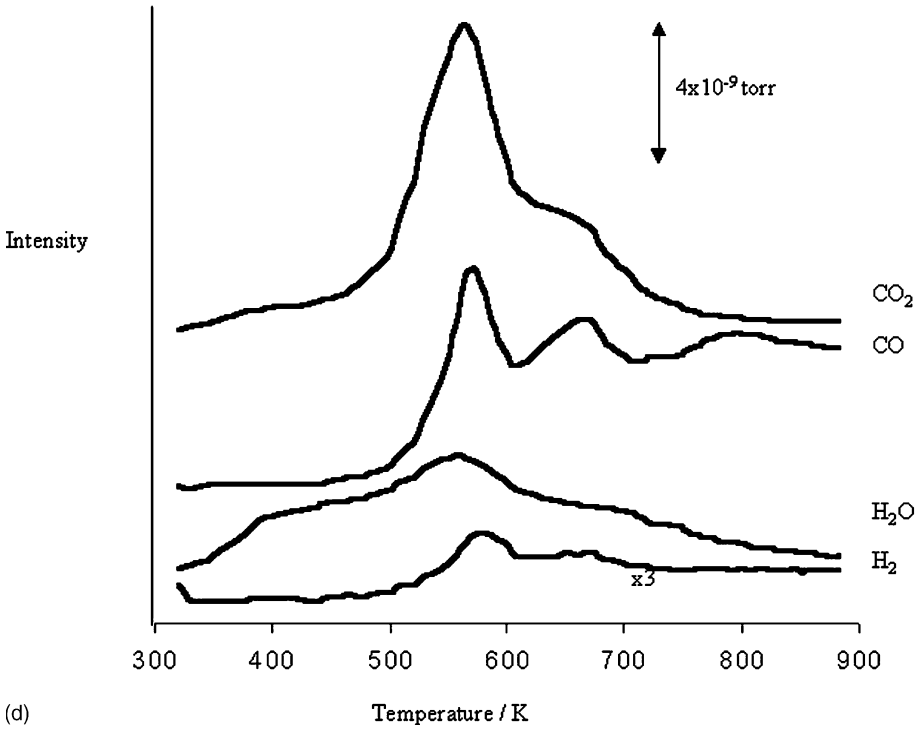

(d)

Fig. 1. (*Continued*).

peaks—a large feature at 420 K and a smaller shoulder at 475 K.

Following adsorption of (*R*,*R*)-tartaric acid on clean Ni{1 1 1} at 350 K, Fig. 1b shows that the desorption of CO, CO_2, H_2O and H_2 occurs in two peaks—a large feature at 440 K and a shoulder at 470 K. The higher adsorption temperature leads to a shift of about 20 K to higher T_{max} in the desorption traces.

When (*R*,*R*)-tartaric acid is adsorbed on Ni{1 1 1}–p(2 × 2)O at 300 K, the desorption traces exhibit a further shift to higher temperature (Fig. 1c). Significantly, there is no H_2 desorption at temperatures below the onset of coincident

CO_2, CO, H_2O and H_2 desorption at 470 K. Instead the only significant desorption below 400 K occurs in the H_2O desorption trace as a shoulder to the main desorption peak. Furthermore, an additional CO desorption state is observed at 580 K.

In Fig. 1d, the desorption traces are shown following a 15 min (*R*,*R*)-tartaric acid dose on Ni{1 1 1}–NiO{1 1 1}. In this case, each trace shows peaks at 570 and 650 K. In addition, a broad low temperature peak exists for H_2O desorption. Furthermore, CO desorption is observed to occur at temperatures higher than 650 K.

In Fig. 2a and b, RAIR spectra are shown for increasing (*R*,*R*)-tartaric acid doses on the Ni{1 1 1}–p(2 × 2)O and the Ni{1 1 1}–NiO{1 1 1} surfaces, respectively. For comparison, the analogous RAIR spectra for the Ni{1 1 1}–(*R*,*R*)-tartaric acid system are shown in Fig. 2c corresponding to adsorption on the clean surface at 300 and 350 K. The data in Fig. 2c have been presented elsewhere [14]. The bands observed and their vibrational assignments are summarised in Table 1. The 1400–1800 cm^{-1} range is key in identifying the adsorption mode of (*R*,*R*)-tartaric acid on metal surfaces [11]. The presence or absence of features at ∼1400 and ∼1600 cm^{-1} (respectively the symmetric and asymmetric stretching frequencies of the carboxylate functionality) and ∼1650–1750 cm^{-1} (>C=O stretching frequency of the carbonyl functionality) aid in the identification of the surface species present. The key features of the presented spectra are as follows. In Fig. 2a, at low (*R*,*R*)-tartaric acid exposures, this important region of the IR spectrum contains bands at 1605 and 1409 cm^{-1}. As the coverage is increased, these bands increase in intensity

Table 1
Assignments of IR bands for (*R*,*R*)-tartaric acid dosed on Ni{1 1 1}–p(2 × 2)O, Ni{1 1 1}–NiO{1 1 1} and Ni{1 1 1} surfaces

Assignment	Ni{1 1 1}–p(2 × 2)O	NiO–Ni{1 1 1}	Ni{1 1 1}
ν (CO)^{atop}	2039		
	2005		
ν (CO)$^{3\text{-foldhollow}}$	1857	1860	1844
	1840		
ν (C=O)^{acid}	1754	1748	1774
		1722	1762
ν (C=O)^{Hbonded}		1658	
ν_{asym} (OCO)	1605	1601	1618
		1581	
ν_{sym} (OCO)	1409	1431	1431
			1428
ν (C–O) ^{acid}	1383	1377	1386
δ (O–H)^{alc}	1365	1371	1375
δ (C–H)	1196	1177	1310
			1185
δ (O–H)^{acid}	1129	1123	1137
ν (C–O)^{alc}	1111	1110	1111
			1083
ν (C–C)			960

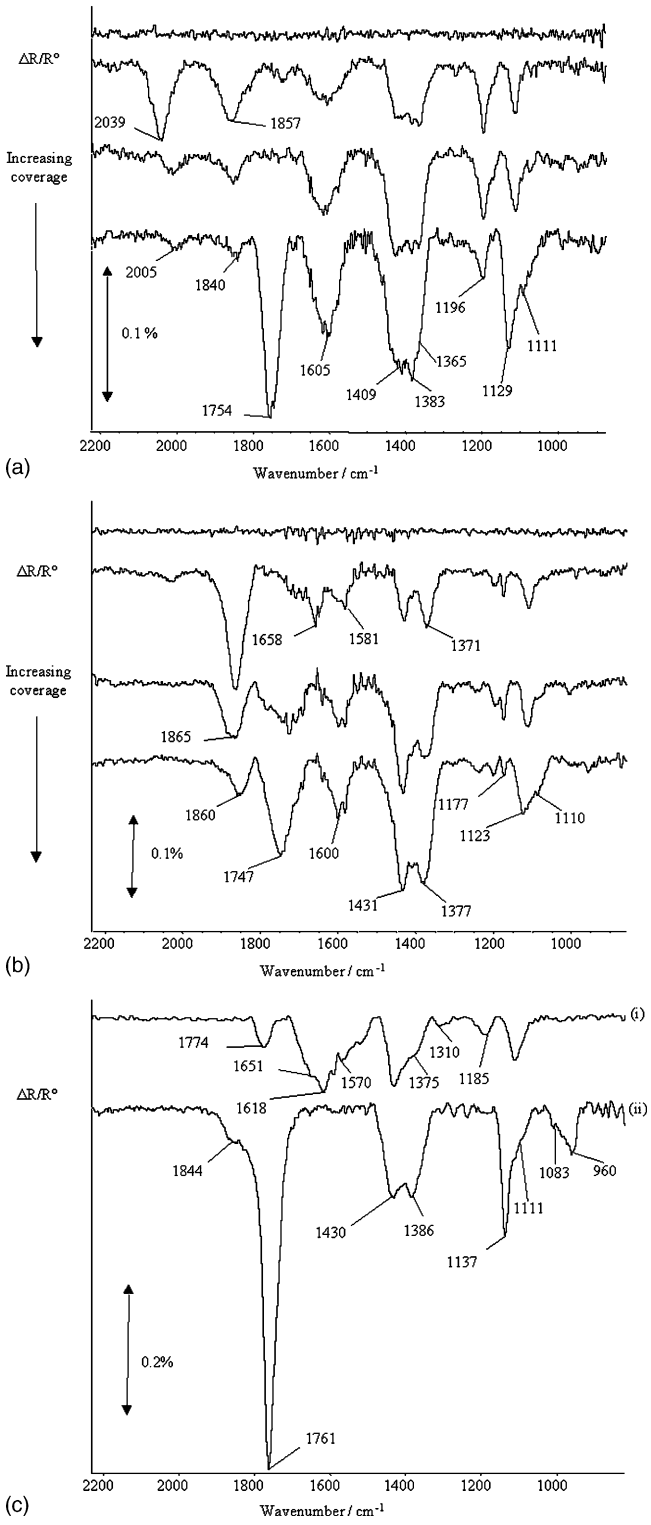

Fig. 2. (a) RAIR spectra for increasing coverage of (*R*,*R*)-tartaric acid on Ni{1 1 1}–p(2 × 2)O at 300 K; (b) RAIR spectra for increasing coverage of (*R*,*R*)-tartaric acid on Ni{1 1 1}-NiO{1 1 1} at 300 K; (c) RAIR spectra for a 900 s (*R*,*R*)-tartaric acid dose on Ni{1 1 1} at (i) 350 K and (ii) 300 K.

and an additional band at 1754 cm^{-1} is observed to grow. In Fig. 2b, bands are observed at 1431 and 1581 cm^{-1} at low coverage. The latter band shifts to 1601 cm^{-1} at high (*R*,*R*)-tartaric acid exposures. At intermediate coverages a peak is observed at 1722 cm^{-1}. This peak is probably still visible at high exposures but now as a shoulder to the peak at 1748 cm^{-1}. In Fig. 2c, the RAIR spectrum for the 300 K (*R*,*R*)-tartaric acid exposure contains peaks at 1428 and 1762 cm^{-1}. The Ni{1 1 1} surface exposed to (*R*,*R*)-tartaric acid at 350 K gives peaks at 1431 and 1774 cm^{-1} and an additional broad feature centred at ∼1618 cm^{-1}. The peaks observed in RAIR spectra in the 1800–2100 cm^{-1} correspond to adventitiously adsorbed CO.

Fig. 3a shows the effect of annealing temperature on the RAIR spectra for the Ni{1 1 1}–p(2 × 2)O–(*R*,*R*)-tartaric acid system. A series of bands appear below 1200 cm^{-1} and there is a general broadening of spectral features in the 1200–1800 cm^{-1} range. The peak at 1755 cm^{-1} is replaced by a more intense feature at 1701 cm^{-1} and there is a shift to higher wave number of the broad peak centred at ∼1400 cm^{-1}. Fig. 3b shows the analagous data for the Ni{1 1 1}–NiO{1 1 1}–(*R*,*R*)-tartaric acid system. In this case, we observe a similar appearance of low frequency bands; the disappearance of the 1747 cm^{-1} band and a general broadening of the features in the 1200–1700 cm^{-1} range.

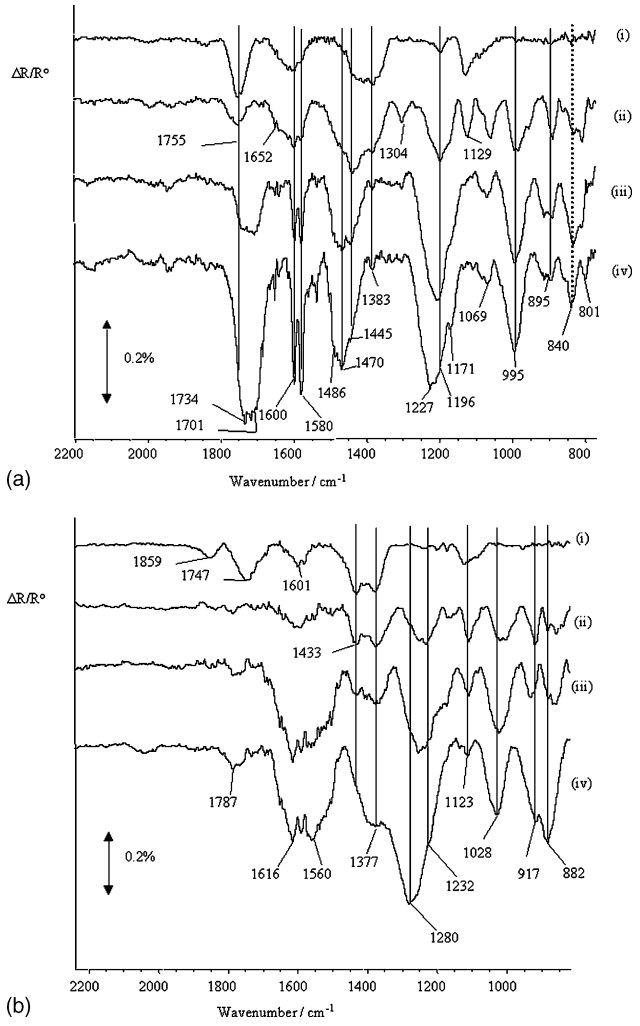

Fig. 3. RAIR spectra on (a) Ni{1 1 1}–p(2 × 2)O and (b) Ni{1 1 1}–NiO{1 1 1} surfaces after (i) 900 s (*R*,*R*)-tartaric acid exposure at 300 K and subsequent annealing to (ii) 323 K, (iii) 373 K and (iv) 423 K.

4. Discussion

The p(2 × 2) oxygen adlayer on Ni{1 1 1} is well known and has been characterised by, for example, Marcus et al. [19] and Caputi et al. [17]. The more severe oxidation treatment results in the formation of a Ni{1 1 1}–NiO{1 1 1} surface. The bulk terminated {1 1 1} face of NiO is thought to be energetically relatively unstable since it consists of alternating layers of Ni^{2+} and O^{2-} ions [20]. To stabilise the surface, the so-called octopolar reconstruction occurs resulting in the formation of a (2 × 2) structure. The reconstruction is thought to occur via the transfer of 1/4 ML of Ni ions from the second layer into positions on the surface of the terminating oxide layer [21]. As a direct consequence of the reconstruction, trigonal pyramids of NiO facets are produced on the surface [16,22]. Exposure of this surface to water (even residual water vapour in a vacuum system) lifts the reconstruction by disrupting the trigonal facets of NiO leading to the formation of close to a monolayer of surface hydroxyl groups [23,24]. The adsorption of formic acid [25] and acetic acid [26] has been studied on Ni{1 1 1}–(2 × 2)-NiO{1 1 1}. These data provide an invaluable reference point for the work contained in this paper on (*R*,*R*)-tartaric acid adsorption. In our case, no attempt was made to deliberately hydroxylate the surface, but LEED showed that the surface consisted of the {1 × 1}-NiO{1 1 1} phase which indicated that the surface was at least partially hydroxylated.

4.1. TPD

A consistent feature of the TPD data is the coincident desorption of CO_2, CO, H_2O and H_2 from the surfaces. This desorption is characteristic of the surface decomposition of adsorbed tartrate species [11,14]. The desorption of CO_2 is analogous to the behaviour observed for simple carboxylate species on a range of metal surfaces (e.g. benzoic acid on Cu{1 1 0} [27]). Presumably the CO, H_2O and H_2 traces are derived from the decomposition of the –CHOH·CHOH– moiety of (*R*,*R*)-tartaric acid. In the absence of preadsorbed oxygen, a low temperature H_2 desorption is observed following (*R*,*R*)-tartaric acid adsorption at 300 K. This peak is derived from the recombination of H species lost in the deprotonation of the COOH functionality of (*R*,*R*)-tartaric acid. When preadsorbed O is present either in the form of O(ads) or as part of a NiO adlayer, the low temperature desorption observed corresponds to the loss of water. It is well known [23,24] that the oxidised surface can react with gas

phase water or acids to produce surface hydroxyl species. It is the decomposition of these species which is the source of H_2O desorption. The higher temperature CO desorption is likely to derive from the recombination of C(ads) formed by the decomposition of tartrate species and oxygen either in the form of O(ads) or oxide ions in the NiO adlayer.

The most interesting feature of the TPD data is the trend in decomposition temperature as a function of the extent of oxidation of Ni{1 1 1}. In addition, the decomposition temperature is shifted to higher temperature by adsorption of (*R*,*R*)-tartaric acid on clean Ni{1 1 1} at 350 K compared with 300 K. The presence of the p(2 × 2)O adlayer has an even greater effect. However, by far the largest effect on the decomposition temperature is observed when the surface is precovered in NiO{1 1 1}. It is interesting to note that the thermal decomposition of bulk nickel(II)tartrate occurs at 650 K [28] which is the same temperature that the smaller coincident desorption trace is observed on Ni{1 1 1}–NiO{1 1 1}. It appears that the more oxidised the Ni surface, the more the adsorption of (*R*,*R*)-tartaric acid results in the surface behaving with comparable thermal stability to nickel tartrate.

A further feature of the TPD spectra is the lack of any "multilayer" desorption peak. It is known from the RAIRS experiments that under the dosing conditions employed molecular tartaric acid species are detected. In other studies on Cu{1 1 0} [11] and Ni{1 1 1} [14] the lack of a multilayer desorption has been interpreted as being due to the (*R*,*R*)-tartaric acid species desorbing at room temperature from the surface. However, the fact that the molecular species are stable at 350 K on the timescale of acquisition of a RAIR spectrum suggests that this species may be simply a precursor which diffuses across the surface until it finds a site in the monolayer to undergo deprotonation and create a direct bond to the metal surface.

4.2. RAIRS

Previous studies of (*R*,*R*)-tartaric acid adsorption on Cu{1 1 0} [11], Ni{1 1 0} [13], Ni{1 1 1} [14] and Ni{1 1 1}/Au [29] have revealed that adsorption can occur via any one of three modes. At sub-ambient temperatures, there is a kinetic barrier to deprotonation enabling the diacid species to exist on the surface. A similar species is observed following room temperature adsorption on Au-rich Ni/Au bimetallic surfaces [29]. At higher temperatures on the more reactive Cu and Ni surfaces and on Ni-rich Ni/Au alloy surfaces either single or double deprotonation can occur enabling adsorption in either the mono- or bi-tartrate configuration. It is thought that the bitartrate conformation is the thermodynamically most stable adsorbed form on Ni [13,14] and Cu [11]. In the case of adsorption of (*R*,*R*)-tartaric acid on the clean Ni{1 1 1} surface at 300 K, only peaks at 1428 and 1762 cm^{-1} were observed. This has been taken to imply the formation of a bitartrate species (1428 cm^{-1}) and a molecular species (1762 cm^{-1}) perhaps accommodated in a second adsorbed layer. The lack of a peak in the 1600 cm^{-1} range shows that the carboxylate species is adsorbed with both oxygen atoms equidistant from the surface. Under these circumstances, the metal surface selection rule allows the symmetric stretching band to be observed but not the asymmetric equivalent since the former has a component of the dynamic dipole moment perpendicular to the surface while the latter vibrational mode has a dynamic dipole moment exclusively parallel to the surface. Adsorbing (*R*,*R*)-tartaric acid at 350 K on Ni{1 1 1} results in a band at ∼1600 cm^{-1} which implies that the carboxylate functionality has an altered geometry where each oxygen atom of the carboxylate is no longer equidistant from the surface. A similar band is observed for (*R*,*R*)-tartaric acid adsorption on both oxygen treated surfaces. In the case of (*R*,*R*)-tartaric acid adsorption on the hydroxylated Ni{1 1 1}–NiO{1 1 1} surface, the observation of the 1600 cm^{-1} band may be related to the fact that the oxide surface consists of trigonal pyramidal facets. In this case, the two oxygens of the carboxylate functionality may be tilted with respect to the {1 1 1} plane due to adsorption on these facets. A similar conclusion was made for the geometry of carbonate on analogous oxidised Ni surfaces by Matsumoto et al. [30].

We will now consider the affect of annealing the tartrate-covered surfaces. The appearance of a series of bands at low frequency and the broadening of the bands in the 1200–1800 cm^{-1} range give the RAIR spectra a very similar appearance to those reported for nickel(II)tartrate [28]. The fact that, compared with the unannealed adlayer, many more bands are observed regardless of the direction of their dynamic dipole moment implies that the annealing treatment results in a relatively random orientation of tartrate species at least consistent with the formation of 3-D crystallites of nickel tartrate.

The trend in decomposition temperature observed when comparing (*R*,*R*)-tartaric acid adsorption on Ni{1 1 1}, Ni{1 1 1}–p(2 × 2)O and Ni{1 1 1}–NiO{1 1 1} can be explained in terms of the nature of the bonding of the carboxylate to Ni. As the surface Ni becomes more oxidised, the interaction energy presumably becomes more favourable as it consists of an electrostatic interaction between Ni^{2+} ions and the negatively charged bitartrate species. In the Ni{1 1 1}–p(2 × 2)O case, the presence of electronegative O atoms presumably causes the neighbouring surface Ni atoms to behave more like $Ni^{\sigma+}$ hence interacting more strongly with adsorbed tartrate. The available space between the O adatoms of the p(2 × 2) structure is quite restricted and may hinder the formation of bitartrate. Indeed, the observation of the peak at 1701 cm^{-1} (ν C=O of the –COO functionality) and the appearance of a band at ∼1450 cm^{-1} (ν C–O of the –COO functionality) suggest that a substantial fraction of the –COO functional groups retain double bond character in one of the C–O bonds. In addition, the lack of a symmetric stretching band of the carboxylate at 1400 cm^{-1} and the presence of bands in the 1600 cm^{-1} range presumably

indicate that some of the –COO functional groups have delocalised electron density but a strongly tilted geometry with respect to the underlying surface such that the symmetric stretching band becomes invisible due to the dipole selection rule. It is not possible to conclude whether this implies two distinct adsorbed species or whether the two ends of the tartrate species are behaving differently.

Even in the NiO{1 1 1} case, the decomposition temperature for the majority of the tartrate species is lower than that for nickel tartrate. This may be related to the fact that the majority of the tartrate species present are in the form of a thin film rather than bulk nickel(II)tartrate.

In terms of surface chemistry, it is likely that, in the partially hydroxylated NiO{1 1 1} case, (*R*,*R*)-tartaric acid reacts with two adjacent OH–Ni^{2+}–OH surface sites forming a bitartrate species bridging two Ni^{2+} ions and liberating two molecules of water. A similar mechanism has been proposed for the adsorption of acetic acid on hydroxylated NiO{1 1 1} [26]. In the octopolar reconstruction of Ni{1 1 1}–(2 × 2)-NiO{1 1 1} the separation of adjacent surface Ni^{2+} ions is ∼5.9 Å [24]. A bitartrate molecule bridging neighbouring nickel ions of this spacing is certainly feasible structurally. It is noteworthy that the Ni–Ni spacing in hydrated nickel(II)(*R*,*R*)-tartrate is 5.2 Å [31]. On heating, the salt adlayer may tend to agglomerate into 3-D crystallites accounting for the change in the RAIR spectra and possibly also the 650 K "nickel(II)tartrate-like" decomposition peak.

4.3. Relevance to enantioselective heterogeneous catalysis

In the preparation of a chirally modified Ni catalyst, one may wish to compare the situation where the surface of the Ni nanoparticles has been exposed to air prior to contact with the modification solution to the case where air has deliberately been excluded prior to the modification process. The former case, we believe, is modelled effectively by the hydroxylated Ni{1 1 1}–NiO{1 1 1} system. In the latter case, surface oxidation of the metallic Ni nanoparticles in aqueous solution will compete in real time with the adsorption of tartrate from solution. While, the UHV preparative routes cannot adequately model interactions at the liquid–solid interface and the important role of, for example, modification pH, we believe that it is not unrealistic to assume that our investigations with less oxidised Ni surfaces may be more pertinent to this situation.

Our conclusion that the surface species produced on modification with (*R*,*R*)-tartaric acid closely resembles nickel tartrate is in agreement with the recent work of Kukula and Cerveny on chirally modified Ni catalysts [28]. The solubility of nickel tartrate in aqueous solution is such that its formation may be the primary factor in the etching of Ni from the surface of Ni nanoparticles during modification. The stronger interaction of tartrate with the initially oxidised Ni particles may facilitate this etching relative to an initially metallic surface. Since etching is achieved by a chiral molecule, one may anticipate that the Ni nanoparticle may be etched such as to reveal chiral arrangements of Ni analogous to the chiral step-kink surfaces such as those described by McFadden et al. [32]. Attard et al. [33] have recently proposed that at least some of the enantioselectivity observed in the Pt catalysed system is derived due to a modifier induced asymmetry in the available step-kink sites on the Pt surface. Attard et al. argue that the adsorption of chiral modifiers in the step-kink sites of a Pt catalyst may occur preferentially at one enantiomeric form of the step-kink leaving the mirror equivalent step-kink available as an active site for chiral hydrogenation reactions [33]. It is also interesting to note that the presence of tartrate anions in solution has recently been reported by Switzer et al. [34] to induce chirality in the structure of copper oxide monolayers grown electrochemically on Au surfaces.

The modification temperature is also known to play a role in determining the ultimate enantioselectivity of the Ni based catalysis [1–5]. Our work has shown that modification at 350 K leads to a more thermally stable adlayer giving a RAIR spectrum showing more resemblance to that of nickel tartrate than the equivalent spectrum following adsorption at 300 K.

It is clear that in the Ni catalysed system, the role of surface oxide/hydroxide should not be ignored when considering the modification of Ni nanoparticles. The surface species produced has a very different thermal stability and conformation when adsorption occurs on Ni{1 1 1}–NiO{1 1 1} than on clean Ni or Cu single crystals.

Our work is a first step towards understanding the nature of the chirally modified surface at the liquid solid interface where the role of modification pH and, perhaps more importantly the role of Na^+ may be crucial.

5. Conclusions

1. The adsorption of (*R*,*R*)-tartaric acid on oxidised Ni surfaces results in the formation of an adlayer whose decomposition temperature is ∼130 K higher than on clean Ni{1 1 1}. The thermal stability of the tartrate adlayer increases both with increasing adsorption temperature and increasing oxidation of the Ni surface.
2. RAIRS data and the temperature of thermal decomposition suggest that for pre-oxidised Ni surfaces, the surface species show a strong resemblance to nickel(II)tartrate.
3. The pre-oxidised Ni surfaces typically used in chiral modification may facilitate etching of Ni from the nanoparticle surface and possibly the production of a chiral array of exposed Ni. The recent results of Attard [33] for the Pt-catalysed system would suggest that the formation of chiral Ni arrangements could, even in the absence of chiral modifiers, be responsible for some of the enantioselectivity observed in the catalytic reaction.

Acknowledgements

TEJ acknowledges the UK Engineering and Physical Sciences Research Council (EPSRC) for the award of Ph.D. studentship. We also thank EPSRC for the award of a research grant (GR/N01514) to support this work. In addition, we are grateful to Professor N.V. Richardson for access to his STM/RAIRS apparatus.

References

[1] B. Sharpless, W. Knowles, R. Noyori, Chem. Br. 37 (2001) 24.
[2] G. Webb, P.B. Wells, Catal. Today 12 (1992) 319.
[3] Y. Izumi, Adv. Catal. 32 (1983) 215.
[4] A. Tai, T. Harada, in: Y. Isawawa (Ed.), Tailored Metal Catalysts, D. Reidel Publishing Company, 1986, pp. 265–324.
[5] A. Tai, T. Sugimura, in: D.E. de Vos, I.F.J. Vankelecom, P.A. Jacobs (Eds.), Chiral Catalyst Immobilisation and Recycling, Wiley-VCH, 2000, Chapter 8, pp. 173–208.
[6] M. Studer, H.-U. Blaser, C. Exner, Adv. Synth. Catal. 345 (2003) 45.
[7] I.M. Sutherland, A. Ibbotson, R.B. Moyes, P.B. Wells, J. Catal. 125 (1990) 77.
[8] J.L. Gland, G.A. Somorjai, Surf. Sci. 38 (1973) 157.
[9] A.F. Carley, M.K. Rajumon, M.W. Roberts, P.B. Wells, J. Chem. Soc., Faraday Trans. 91 (1995) 2167.
[10] J.M. Bonello, F.J. Williams, R.M. Lambert, J. Am. Chem. Soc. 125 (2003) 2723.
[11] M. Ortega Lorenzo, S. Haq, T. Bertrams, P.W. Murray, R. Raval, C.J. Baddeley, J. Phys. Chem. B 103 (1999) 10661.
[12] M.O. Lorenzo, C.J. Baddeley, C. Muryn, R. Raval, Nature 404 (2000) 376.
[13] V. Humblot, S. Haq, C. Muryn, W. Hofer, R. Raval, J. Am. Chem. Soc. 124 (2002) 503.
[14] T.E. Jones, C.J. Baddeley, Surf. Sci. 513 (2002) 453.
[15] T.E. Jones, C.J. Baddeley, Surf. Sci. 519 (2002) 237.
[16] F. Rohr, K. Wirth, J. Libuda, D. Cappus, M. Baumer, H.-J. Freund, Surf. Sci. 315 (1994) L977.
[17] L.S. Caputi, S.L. Jiang, A. Amoddeo, R. Tucci, Phys. Rev. B 41 (1990) 8513.
[18] M.A. Langell, M.H. Nassir, J. Phys. Chem. 99 (1995) 4162.
[19] P.M. Marcus, J.E. Demuth, D.W. Jepsen, Surf. Sci. 53 (1975) 501.
[20] A. Barbier, G. Renaud, Surf. Sci. 392 (1997) L15.
[21] N. Erdman, O. Warschkow, D.E. Ellis, L.D. Marks, Surf. Sci. 470 (2000) 1.
[22] M. Schonnenbeck, D. Cappus, J. Klinkmann, H.-J. Freund, L.G.M. Petterson, P.S. Bagus, Surf. Sci. 347 (1996) 337.
[23] J.C. de Jesus, J. Carrazza, P. Pereira, F. Zaera, Surf. Sci. 397 (1998) 34.
[24] N. Kikatsu, V. Maurice, C. Hinnen, P. Marcus, Surf. Sci. 407 (1998) 36.
[25] T. Matsumoto, A. Bandara, J. Kubota, C. Hirose, K. Donnen, J. Phys. Chem. B 102 (1998) 2979.
[26] M.A. Langell, C.L. Berrie, M.H. Nassir, K.W. Wulser, Surf. Sci. 320 (1994) 25.
[27] Q. Chen, C.C. Perry, B.G. Frederick, P.W. Murray, S. Haq, N.V. Richardson, Surf. Sci. 446 (2000) 63.
[28] P. Kukula, L. Cerveny, Appl. Catal. A: Gen. 223 (2002) 43.
[29] T.E. Jones, T.C.Q. Noakes, P. Bailey, C.J. Baddeley, J. Phys. Chem. B 108 (2004) 4759.
[30] T. Matsumoto, J. Kubota, J.N. Kondo, C. Hirose, K. Domen, Langmuir 15 (1999) 2158.
[31] L.J. Bostelaar, R.A.G. de Graaff, F.B. Hulsbergen, J. Reedijk, W.M.H. Sachtler, Inorg. Chem. 23 (1984) 2294.
[32] C.F. McFadden, P.S. Cremer, A.J. Gellman, Langmuir 12 (1996) 2483.
[33] G.A. Attard, J.E. Gillies, C.A. Harris, D.J. Jenkins, P. Johnston, M.A. Price, D.J. Watson, P.B. Wells, Appl. Catal. A: Gen. 222 (2001) 393.
[34] J.A. Switzer, H.M. Kothari, P. Poizot, S. Nakanishi, E.W. Bohannan, Nature 425 (2003) 490.